Evaluation of semi-mechanistic models to predict soil to grass transfer factor of 137Cs based on long term observations in French pastures

Khaled Brimo, Laurent Pourcelot, Jean Michel Metivier

Evaluation of semi-mechanistic models to predict soil to grass transfer factor of ^{137}Cs based on long term observations in French pastures

Khaled Brimo[a]*, Laurent Pourcelot[a], Jean Michel Métivier[a], Marc André Gonze[a]

[a] Institut de Radioprotection et de Sûreté Nucléaire (IRSN), LEREN, Cadarache, 13115 Saint Paul lez Durance, France

*Corresponding authors: Khaled BRIMO

Tel: + 33 04.42.19.91.09

E-mail: khaledbrimo@gmail.com

Abstract

The aim of this study was to evaluate and improve the accuracy of the semi-mechanistic models used in regulatory exposure assessment tools, to describe the transfer factors (*TF*) of ^{137}Cs from pasture soils to grass observed in different grazing areas of France between 2004 and 2017. This involved a preliminary parameterization step of the dynamic factor describing the ageing of radiocesium in the root zone using a Bayesian approach. A data set with mid-term (10 years about) and long term (more than 20 years) field and literature data from 4 European countries was used. A double kinetics of the bioavailability decay was evidenced with two half-life periods equal to 0.46±0.11 yr and 9.57±1.12 yr for the fast and slow declining rates respectively. We, then, tested a few existing alternative models proposed in literature. The comparison with field data showed that these models always underestimated the observations by one to two orders of magnitude, suggesting that the solid-liquid partition coefficient (*Kd*) was overestimated by models. The results suggest that semi mechanistic models might fail in the long-term prediction of the radionuclide transfer from soil-to-plant in the food chain. They highlight the need to calculate *Kd* using easily exchangeable ^{137}Cs (i.e. labile fraction) rather than total soil ^{137}Cs.

Keywords: Cesium 137, Bioavailability, Chernobyl and global fallout, Absalom model, Parameter estimation, Uncertainty

1. Introduction

During the last two decades, numerous radioecological models have been developed to predict the soil-to-plant transfer of radiocesium (^{137}Cs) in pastures contaminated by atmospheric fallouts (Absalom et al., 2001; Wright et al., 2003; Yamamura et al., 2018). A better quantitative understanding of food-chain transfers is of primary importance when assessing the radiation exposures and doses to man, notably in case of a nuclear accident. Models essentially differ in the level of complexity adopted in both the conceptual description of the soil-plant system (e.g. features, events and processes) and the mathematical parameterization of the biological and physic-chemical mechanisms considered (Almahayni et al., 2019). One of the simplest approaches is the well-known Transfer Factor approach (IAEA-TECDOC-472, 2010) which fails to explain the observed variability. More elaborated approaches have been developed which try to explicitly account for the influence of some important environmental characteristics (e.g. soil properties) through semi-mechanistic parameterizations. Examples of semi mechanistic approaches are the models published by Absalom et al. (2001), Tarsitano et al. (2011) and Uematsu et al. (2015) which enable to assess the transfer of cesium based on some soil properties (e.g. clay content, organic matter content, exchangeable potassium) and the time elapsed since the initial deposit. These models explicitly take into account the phenomena associated with the decrease of ^{137}Cs bioavailability during the years following the deposition phase by introducing a dynamic factor depending on the time elapsed since the deposition date. Special attention should be paid to its estimation since its value may drastically influence the predicted activity in plants.

Despite findings indicating that bioavailability of radiocesium in soil decreases with time (Absalom et al., 1995; Brimo et al., 2019; Smith et al., 1999), these models have been often developed and tested against data sets mostly limited to laboratory experiments on relatively short time scales (i.e. from a few days to a few years) .Thus, the validity of these models

under real field conditions and on longer time scales (i.e. several decades after an accident) is highly questionable. Additionally, the uncertainties associated to the model parameters and their impacts on model predictions have not been addressed in the literature. The main objective of the present work was to evaluate the performance of these semi-mechanistic models by comparing the predicted soil-to-pasture vegetation transfer factors with field observations acquired in French pastures on the long term (i.e. 20 to 30 years after Chernobyl and 50 years after global fallout). Such an objective also implies to more reliably quantify the bioavailability decay rates on both mid and long terms after deposition, and their respective contributions. This was accomplished by calibrating these constants against mid-term (10 years about) and long term (more than 20 years) field and literature data acquired after Chernobyl accident in several European countries, based on a Bayesian approach.

2. Material and methods

2.1. Model descriptions

The simplest approach to quantify the soil-to-grass vegetation transfer of radiocesium in pastures relies on the use of an aggregated transfer coefficient T_{ag} (in m^2/kg) which quantifies the activity concentration in grass vegetation in (Bq/kg) normalized by the activity inventory in soil (in Bq/m^2) (IAEA-TECDOC-472, 2010). This definition can also be extended to cow's milk in the considered ecosystem (i.e. soil-to milk aggregated transfer factor). One major drawback of this approach is the large spatial variability of T_{ag} values - even on a small area - due to the quite inhomogeneous ^{137}Cs deposition patterns. In addition to spatial variability, a decrease of T_{ag} values over time was often observed as a result of the decrease of cesium availability in the root soil due to both its irreversible fixation on soil particles and its migration down through the soil profile (Albers et al., 2000; IAEA-TECDOC-472, 2010). These lead thus to a substantial over or underestimate of the predicted risk, and therefore this

92 approach was not used in this work. An alternative approach to quantify the soil-to-grass
93 transfer of radiocesium in pastures relies on the use of a soil-to-grass transfer factor TF
94 (dimensionless), defined as the ratio between the radioactivity concentration in grass (C_V in
95 Bq/kg_{dm} where dm denotes to dry mass) to that in the root soil layer (C_S in Bq/kg_{dm}) (see
96 equation (1) below). This approach is only valuable when the contribution of the foliar
97 pathway becomes negligible and the uptake by roots is the major process controlling the
98 radionuclide activity concentration in grass. It is usually assumed that TF is constant with
99 time, although its value is tabulated for different groups of soils and plants (IAEA-TECDOC-
100 472, 2010):

$$TF = \frac{C_V(t)}{C_S(t)} = cte \qquad (1)$$

101 Using equation (1), it is possible to predict the radiocesium concentration in grass at any time
102 (t) recognizing the tabulated TF value and the radioactivity concentration in the root layer of
103 soil. To refine the approach, Absalom et al. (1999) proposed in their model to partition the
104 ^{137}Cs content in the root layer into two fractions : a non-bioavailable one that evolves over
105 time and another bioavailable that contains radiocesium in both solute and solid forms (the
106 concentrations of which are assumed at instantaneous reversible equilibrium). The predicted
107 TF at time t (in years) is further decomposed as follows:

$$TF(t) = \frac{C_V(t)}{C_S(t)} = \frac{CF}{Kd}.D(t) \qquad (2)$$

108 This approach requires the determination of two empirical parameters independent of time:
109 the solid liquid distribution coefficient Kd (in L/kg_{dm}) and the concentration factor CF (in
110 L/kg_{dm}) defined as the ratio of activity concentration in grass vegetation to that in soil
111 solution. The calculation of Kd and CF requires knowledge of some soil physico-chemical
112 properties. An additional dynamic factor, namely $D(t)$ (dimensionless), representing the

ageing of ^{137}Cs in the rooting layer, is defined as the percentage of bioavailable ^{137}Cs with respect to time. Bioavailability is decreasing over time (D ranging from 0 to 1) mainly due to the fixation onto soil particles (Smith et al., 1999). Here, the decreasing of D is quite independent of loss factors such as radioactivity decay, water removal (leaching, run-off), erosion and removal of harvested biomass since all these factors are already implicitly taken into account through time dependent of ^{137}Cs.

2.1.1. Parameterization of D(t)

According to IAEA report (IAEA-TECDOC-472, 2010), the bioavailable fraction $D(t)$ can be neglected (i.e. sets equal to 1) when comparing TF for a set of similar soils on mid-term after a contamination event. However, this assumption might be invalid when predicting the long term behavior of radiocesium. In their model, Absalom et al. (1999) assumed that the decrease of bioavailability depends on the time elapsed between the date of observation (t) and the date of the initial deposition (t_0), and therefore on the age of contamination in soil (t-t0). More precisely, the bioavailable fraction D depends only on ($t-t_0$). D is, therefore, supposed to be "invariant with time" since it does not depend on t_0 but rather on ($t-t_0$). They also assumed that the decrease of bioavailable radiocesium in soil was characterized by two consecutive fast and slow rates described by a first order kinetic equation. In the case of a single contamination episode taking place on date t_0, D(t-t0) is given by equation (3):

$$D(t-t_0) = P_{fast}.\exp\left(-k_{fast}.(t-t_0)\right) + \left(1-P_{fast}\right).\exp\left(-k_{slow}.(t-t_0)\right) \quad (3)$$

Where, k_{fast} and k_{slow} (in yr^{-1}) are the apparent first order kinetic rates for the fast (P_{fast}) and the slow ($1-P_{fast}$) declining fractions, respectively. P_{fast} represents the fraction of the (initially bioavailable) deposited radiocesium which is subject to decay according to the fast component. However, in the case of French pastures which were contaminated by both the

Chernobyl accident in 1986 and the global fallouts of nuclear weapons testing in the 1960s, this formulation has to be extrapolated. When ^{137}Cs is introduced into soil by two consecutive contamination events occurring at times t_1 and t_2 respectively, the equation (3) can be rewritten as follows:

$$D(t) = \vartheta . D(t - t_1) + (1 - \vartheta) . D(t - t_2) \qquad (4)$$

Where, ϑ (ranging from 0 to 1) quantifies the contribution of Chernobyl fallout to the total deposit at the considered site and $D(t\text{-}t_1)$ and $D(t\text{-}t_2)$ are calculated according to equation (3). As a result of the time invariance hypothesis (i.e. soil structure and properties do not vary significantly over time), it is reasonable to consider that the values of P_{fast}, k_{fast} and k_{slow} constants do not change between the two contamination events.

To date, there is very little data in literature on P_{fast}, k_{fast} and k_{slow} values and their associated uncertainties due to lack of observed data. In this work, we chose to evaluate these kinetic constants using mid and long-term field and literature chronic series of radiocesium in milk observed after Chernobyl accident. Indeed, such data are scarce in literature and unavailable for grass. Here our calculations were based on the hypothesis reported in literature that the radiocesium activity concentration in milk at mid and long terms can change at the same rate as the activity concentration in grass which in turn is in equilibrium with the radiocesium concentration in soil solution (Smith et al., 1999; Absalom et al., 1999; Brimo et al., 2019).

Mathematically, the rates of change in the radiocesium content of *vegetation pasture or cow s' milk* (M) can be expressed as follows:

$$\frac{C_M(t)}{C_{M,t0}} = P_{fast} . \exp\left(-\left(\lambda_{fast}^M + \lambda\right) . t\right) + \left(1 - P_{fast}\right) . \exp(-(\lambda_{slow}^M + \lambda) . t) \qquad (5)$$

Where C_M is the total activity concentration in M at time t, $C_{M,t0}$ denotes the initial radiocesium concentration in M after the very short-term transfer processes such as atmospheric deposition and weathering of radiocesium intercepted by vegetation are were ceased. λ is the physical decay rate (2.31×10^{-2} yr $^{-1}$), P_{fast} is the same as that involved in Eq. 3 and λ_{fast}^{M} and λ_{slow}^{M} are the fast and slow decline rates (physical decay excluded) for the fast and slow declining fractions respectively, mainly caused by the combined effects of the radiocesium fixation on specific and non-specific sites, the leaching of the upper rooting layer by downward infiltration, the soil erosion and the grazing consecutive to grass uptake (Brimo et al., 2019). On the other hand, the rates of change in the total radiocesium content of soil (i.e. the sum of bioavailable and non-bioavailable fractions) are usually described by assuming that the decline in radioactivity concentration, C_S, is exponential (i.e. $C_s \propto \exp(-(\lambda^{soil}+\lambda).t)$). λ^{soil} is subject to the same aforementioned loss processes as λ_{fast}^{M} and λ_{slow}^{M} excluding the fixation contribution. Here, if the contribution of the environmental processes other than physical decay is small compared to the contribution of fixation, C_S would then change with a single rate close to the physical decay (i.e. $\lambda^{soil} = \lambda_{fast}^{soil} = \lambda_{slow}^{soil}$). Thus, based on above analysis, we first determined the values of the 3 constants ($P_{fast}, \lambda_{fast}^{M}, \lambda_{slow}^{M}$) by analyzing the decrease of radiocesium activity in milk (i.e. *M=milk*) observed in several European countries (see section 2.2.2). The constants of the bioavailable fraction k_{fast} and k_{slow} required in Eq. 3 were then deduced as follows:

$$k_{fast} = \lambda_{fast}^{milk} - \lambda^{soil} \qquad (6)$$

$$k_{slow} = \lambda_{slow}^{milk} - \lambda^{soil} \qquad (7)$$

175 *2.1.2. Parameterization of CF and Kd*

176 Calculation of *CF* and *Kd* relies on the knowledge of soil properties including clay content,
177 pH, organic matter content (OM), cation exchange capacity (CEC) and exchangeable
178 potassium (K) concentration. In the present work, the calculation of *CF* was performed by
179 testing different semi-mechanistic formulations derived by Smolders et al. (1997), Absalom
180 et al. (1999), Absalom et al. (2001) or Tarsitano et al. (2011). Similarly, the parameter *Kd* was
181 estimated based on one of the following models: Absalom et al. (1999), Absalom et al. (2001)
182 , Tarsitano et al. (2011) or Uematsu et al. (2015). The sets of mathematical equations with
183 their default parameter values are summarized in Supplementary Information (SI). These
184 equations differ by their mathematical formulation, the required input soil properties and also
185 by the type of soils for which they were developed. While the equation of Uematsu et al.
186 (2015) was mainly derived using agricultural Japanese soils from the Fukushima affected
187 areas, all other equations were derived on the basis of data mostly acquired in laboratory
188 experiments. These latter were carried out on mineral soils collected from European
189 grasslands and have lasted over periods of several weeks to several months (i.e. the cases of
190 Absalom et al. (1999) and Smolders et al. (1997)). However, in addition to the mineral soils,
191 the equations given by Absalom et al. (2001) and Tarsitano et al. (2011) were parameterized
192 using additional field data obtained for soils with high organic matter contents.

193 **2.2. Field data**

194 *2.2.1. Data used for calibrating D(t)*

195 As listed in Table 1, it consists of 10 different long term monitoring series of ^{137}Cs activity
196 concentrations in cow's milk, mostly acquired in grazing areas in France. The data acquired in
197 France were for a part already described in Brimo et al. (2019) and for the other part
198 unpublished (i.e. Puy de Dôme). To enrich the dataset, we further included time series of the
199 aggregated transfer coefficients (T_{ag}) of ^{137}Cs activity in milk acquired from 1986 to 1999 in

three other European countries (Austria, Czech Republic and Germany) and compiled in Mück (2003). Overall, we had access to about 200 measurements that covered the entire period from 1986 to 2017.

Table 1: Description of the milk time series used to estimate the values of P_{fast}, k_{fast} and k_{slow}

Source	Location	Observation period	Nb. of observations (*n*)
Mück (2003)	Austria	1986-1999	12
	Germany	1986-1999	12
	Czech Republic	1986-1999	14
This study	France Puy de Dôme	1986-1999	52
Brimo et al. (2019)	Beaune-le-Froid	1993-2016	22
	Crey-Malville	1996-2016	14
	Cruas	1994-2016	18
	Tricastin	2000-2015	10
	Chooz	1992-2016	24
	Mercantour	1999-2017	18

2.2.2. Data used for testing *TF* models

The data set selected for testing *TF* model performances is independent from that used for estimating the bioavailability decay constants in the previous section. The model performances were evaluated against data acquired in different grazing areas in France. Overall, 101 pasture soils were sampled from 2004 to 2017. Most soils originated from two areas: Jura (56 samples from 9 monitoring stations) and Puy de Dôme (19 samples from 3 monitoring stations) located respectively in eastern and central part of France. The 26 other

soil samples were taken in the vicinity of some nuclear power plants (the soil samples not originated from Puy de Dôme or Jura are denoted NPP hereafter), in the course of radiological monitoring programs carried out by IRSN. The contribution of the NPP releases to the contamination of soils in these areas was considered negligible (Duffa et al., 2004), the main sources remaining, as underlined before, the Chernobyl accident and the nuclear tests. In addition to the soil physicochemical properties, ^{137}Cs activity concentration was determined in the upper soil (0-5 cm) and grass (stems and shoots) from which we calculated the transfer factors. Methodologies adopted for sampling, preparation of samples and ^{137}Cs analyses are detailed in a previous work (Brimo et al., 2019).

Table S3 in SI shows in details sampling date, location, observed *TF* and the physiochemical properties (pH, clay content, organic matter content, cation exchangeable capacity, exchangeable K) of the 101 soil samples. The values of the observed ^{137}Cs in soil ranged from 2.3 to 103 Bq/kg, the observed ^{137}Cs in grass from 0.045 to 13.9 Bq/kg, the clay content from 0.05 to 0.56 g/g, the organic matter content from 0.02 to 0.44 g/g, the pH in soil solution from 4.4 to 7.7, the exchangeable K from 0.04 to 2.53 cmol/kg and the CEC from 0.42 to 50.3 cmol/kg. In Puy de Dome, the soil was loamy with high organic matter content (i.e. OM $\geq$ 20%) whereas it was loamy with low OM content in NPP sites. In the Jura region, the soil varied between organic (16%), loamy (29%) and clay soils (55%) (IAEA classification (IAEA-TECDOC-472, 2010)).

2.3. Modelling methodology

2.3.1. Determination of the bioavailability factor constants

Based on the hypothesis of the independence of the bioavailability decay constants (P_{fast}, k_{fast}, k_{slow}) upon the considered site, two different approaches were used to determine them. In the first approach, the determination was accomplished by considering only the relatively short time series extending from 1986 to 1999 (i.e. Austria, Germany, Czech Republic and Puy de

239 Dôme). In the second approach, we took into account all the series in order to evaluate the
240 influence of long term data on the estimates. In order to avoid any bias in the results, we
241 ignored ^{137}Cs measurements recorded in 1986 since they were considered highly impacted by
242 the foliar uptake pathway. On the other hand, we took into account the variability of the initial
243 activity levels between sites since they were not contaminated at the same deposit level. We
244 chose to treat the initial activity levels (i.e. $C_{M,t0}$) for every selected time series as extra
245 constants and they were, therefore, adjusted simultaneously with the bioavailability constants.
246 Consequently, 7 constants (i.e. P_{fast}, k_{fast}, k_{slow} + 4 initial activity levels of the used chronic
247 time serries) needed to be determined in the first approach versus 13 (3+10) in the second
248 approach. To fit the values of these constants, we implemented equations 5, 6 and 7 in
249 Matlab. The value of λ^{soil} that is required for deduction k_{fast} and k_{slow} values was set to
250 0.017±0.005 yr^{-1} taken from our former work (Brimo et al., 2019). We used the algorithm
251 DREAM based on the Bayesian approach to fit the whole constants with their associated
252 uncertainty. DREAM uses adapted Markov chain Monte-Carlo method that exhibits excellent
253 sampling efficiencies on high dimensional posterior distributions (Vrugt, 2016). An
254 aggregated logarithmic mean square error as described by Brown and Dvarzhak (2019) was
255 chosen as a likelihood function. The algorithm was run with uniform prior distributions
256 (Table 2). The initial time (t_0) was set to May 01, 1986, and was assumed to be the beginning
257 of ^{137}Cs deposit for all sites. Except for Puy de Dôme, the constants P_{fast}, k_{fast} were set to zeros
258 (i.e. prior=posterior=0) for all French time series because these did not exhibit any rapidly
259 decaying fraction as they started in the early 1990's (i.e. more than 6 years after Chernobyl).

260 *2.3.2. Calculation of TFs with semi-mechanistic models*

261 Based on the estimated values of the bioavailability decay constants (mean ± SD) and the
262 correlations in-between them, the soil-to-plant transfer factor was calculated for each of the
263 101 samples through Monte-Carlo simulations (2.5 x 10^5 runs), taking into account

uncertainties in *D*, *CF* and *Kd*. The simulations were run by setting the Chernobyl deposit (t_1) to May 01, 1986, whereas the global fallout (t_2) was assumed uncertain with a deposition date being uniformly randomly distributed between January 01, 1960, and December 31, 1965, since most of atmospheric deposits had occurred by that period (Renaud and Louvat, 2004) . The values of ϑ (mean ± SD) were derived from maps provided by Roussel-Debet et al. (2007) (Table S3 in SI). Each ϑ value represents the arithmetical mean of ϑ values taken within area delineated by a circle having a diameter of 30 km around the sampling coordinates. Indeed, theses maps are reliable at regional scales but much less reliable at smaller spatial scales, for kilometric to deca-kilometric scales. This is why we chose such a diameter to be big enough but with avoiding overlapping between two adjacent circles. Simulations with ϑ values derived from 60 km circles were also carried out for comparison purpose but the final results did not show any difference. *CF* and *Kd* values were estimated using different alternative models or combinations of models. : In addition to the 3 classical models (i.e. M1, M2, M3) of Absalom et al. (1999), Absalom et al. (2001) and Tarsitano et al. (2011), 3 other alternatives (i.e. M4, M5, M6) were tested by using the equation of Smolders et al. (1997) to estimate *CF* while keeping the calculation of *Kd* according to the 3 previous classical original models. Three other alternatives (i.e. M7, M8, M9) were performed by calculating *Kd* on the basis of the RIP^{soil} (i.e. Radiocesium Interception Potential in soil) equation reported by Uematsu et al. (2015) while keeping the calculation of *CF* according to the 3 previous classical models. Consequently, 9 different models were tested.

2.3.3. Assessment of the model performances

In order to quantitatively assess model performances, the difference between the predicted and observed *TFs* were quantified by the following statistical indexes: the correlation coefficient (*r*) using log transformed data, the *Contained* index (%) by calculating the percentage of observed data inside the predicted bounds and the predicted-to-observed value

ratio denoted $\overline{sim}/obs$. The latter was calculated as follows: the ratio of the predicted median value to the observed one was first calculated for each sample, from which a median ratio was calculated. The best performance is assessed by: a close to ±1 *r* values, close to 100 % *Contained* values and close to 1 ratio $\overline{sim}/obs$ values.

3. Results and discussion

3.1. Bioavailable fraction constants

XXX Table 2 compares the estimates of the posterior mean (Mean) and standard deviation (SD) of P_{fast}, k_{fast} and k_{slow} constants for the two approaches. The corresponding posterior cumulative distribution functions (CDFs) are displayed in Fig 1. The posterior CDFs are well defined and occupy small ranges within the uniform prior distributions, suggesting that the data used included sufficient information to calibrate *D*. This is also confirmed by the nearly Gaussian distributions of k_{fast} and k_{slow}. The distribution of P_{fast} appears to depart from Gaussian and concentrates at its upper possible bound (Fig 2). Results show that k_{fast} and k_{slow} given by approach 2 were 1.2-1.3 times higher than that given by approach 1 (Table 1). However, taking the uncertainties associated with constants into account, this difference seems slight and is due to difference in the selected time series used as calibration data. The effective mid-term half-lives $\left(\frac{\ln 2}{k_{fast}+\lambda}\right)$ amount to 0.59±0.12 yr for approach 1 and 0.46±0.11 yr for approach 2, while the effective long-term half-lives $\left(\frac{\ln 2}{k_{slow}+\lambda}\right)$ amount to 12.05±4.88 yr and 9.57±1.12 yr, respectively. The ratio k_{fast}/k_{slow} is approximately the same for the two approaches, i.e. 31 and 32. The relatively short half-lives estimated for the fast component suggests that fixation of the bioavailable ^{137}Cs starts during the first few weeks to months after initial deposition. This finding is consistent with the opinion of Frissel et al. (2002) who concluded that 1 year could be enough for ^{137}Cs fixation in soil. Both approaches give a very

high value around 0.97 for the fast-declining fraction (P_{fast}) which means that ^{137}Cs bioavailability for the investigated soils has decreased drastically within 2 years after the accident. Our constant estimations differ from the very few values reported in literature. Tarsitano et al. (2011) dropped out the rapid term (i.e. P_{fast}=k_{fast}=0) from their version of equation (3) arguing that this term was not necessary. However, their hypothesis seems not realistic in our case since the two decline phases are obvious for European soils contaminated by Chernobyl fallouts (Fig. 2). Our findings of k_{fast} and k_{slow} are respectively 1.8-2.3 times higher and 0.6-0.7 times lower than the corresponding values reported by Absalom et al. (1999) (i.e. k_{fast} and k_{slow} of 0.69 and 0.069 yr^{-1} respectively). Furthermore, these authors estimated a value of 0.81 for P_{fast} which is far away from the lower end of the range of values obtained by the present study (see Fig 1). A possible reason of this lower P_{fast} value is that Absalom et al. (1999) chose to optimize this single parameter using imposed values for k_{fast} and k_{slow} despite the correlation among the three parameters (e.g. r= 0.8 between P_{fast} and k_{fast}). Another possible reason is that P_{fast} value reported by Absalom and co-authors might have been estimated based on data impacted by foliar uptake. Indeed, two of the data sets used in P_{fast} optimization involved data observed in 1986, soon after Chernobyl accident (see Table 1 in Absalom et al. (1999)).

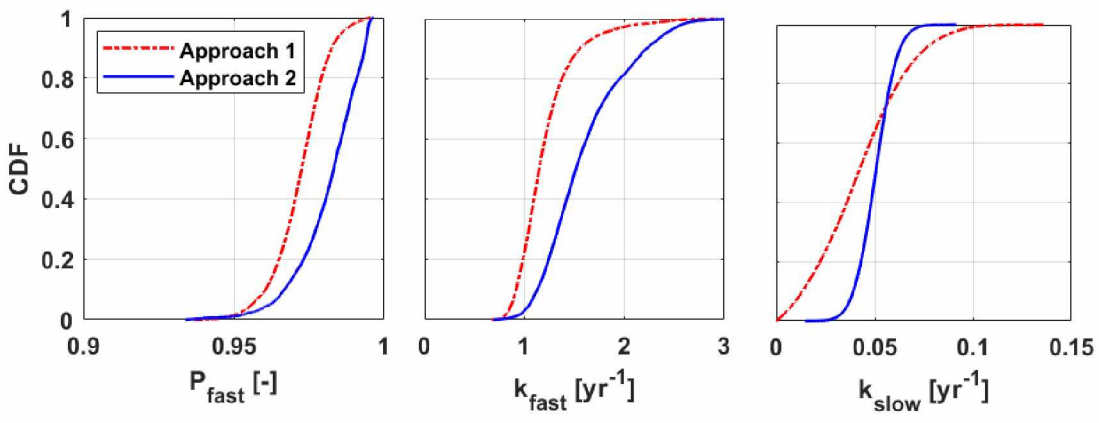

Fig 1: Posterior CDFs of P_{fast}, k_{fast} and k_{slow} parameter values given by the two calibration approaches.

Table 2: Mean and standard deviation (SD) values of the bioavailability decay constants derived by the two calibration approaches.

Parameter	Unit	Searching range	Approach 1		Approach 2	
			Mean	SD	Mean	SD
P_{fast}	-	[0-1]	0.97	0.009	0.98	0.011
k_{fast}	yr^{-1}	[0-6]	1.21	0.263	1.60	0.416
k_{slow}	yr^{-1}	[0-1]	0.043	0.022	0.050	0.009

The comparison between the observed and the predicted activity concentrations in cow's milk based on calibrated constants are displayed in Fig 2 for the two calibration approaches mentioned above. Satisfactory fits to the observed data were found for both approaches, with *r* values varying between 0.69 (n=24) and 1 (n=12) with values being greater than 0.8 for all 1986-1999 time series. The observations of these latter confirm the hypothesis of a two-phase decrease with time. Despite different environmental conditions, the decay rates observed in France (Puy de Dôme), Germany, Czech Republic and to some extent in Austria are very similar as illustrated by the near-parallel lines of decreasing radioactivity concentrations in cow's milk (Fig 2). This was statistically validated with ANOVA, Turkey's multiple comparison analysis tests. For this purpose, the previous constants were calibrated for each single country individually (results not shown). The *p* values yielded by the statistical test indicated no significant difference between the four European countries (*p*-values of 0.42, 0.15 and 0.59 for P_{fast}, k_{fast} and k_{slow} respectively). Therefore, our results indicate that literature data do not call into question the present assumption that bioavailability decay constants can be considered as site-independent.

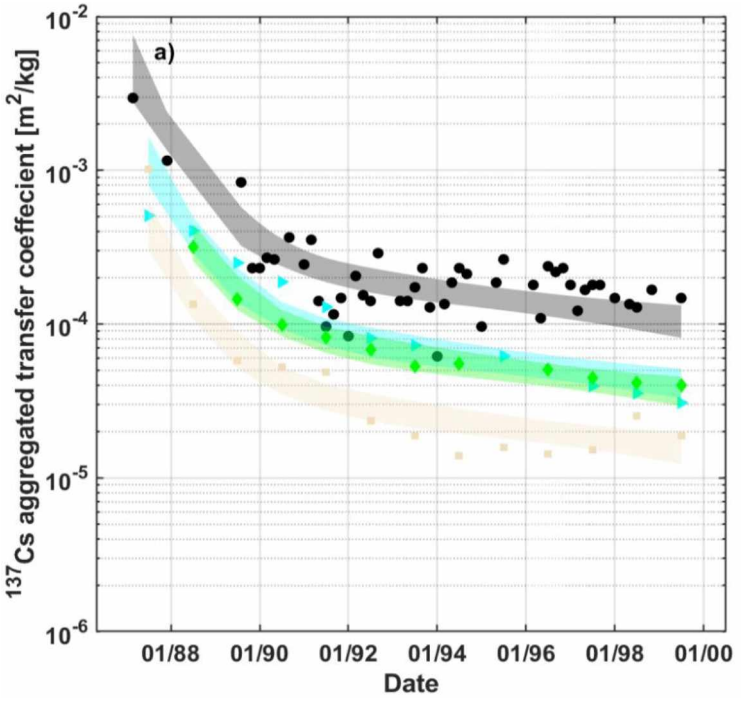

353

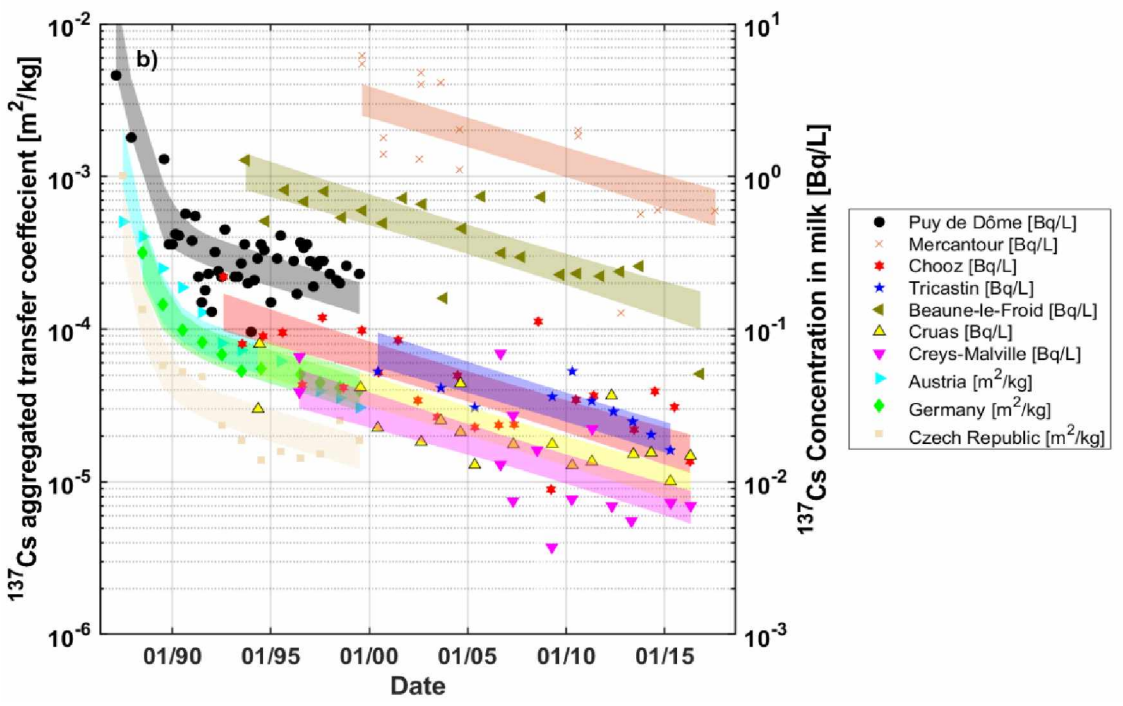

354

355 **Fig 2**: Comparison between observed (symbols) and predicted (line) values of the ^{137}Cs activity
356 concentration in cow milk (normalized by the deposit for Austria, Germany and Czech Republic): (a)
357 with long-term time series excluded (approach 1), (b) with all series being considered (approach 2).

358 Based on the above discussion and taking into account that the semi-mechanistic models will
359 be tested against field data acquired 20 to 30 years after Chernobyl accident, we chose to

360 calculate the bioavailability decay D using the decay constants given by approach 2. The time
361 evolution of the predicted bioavailability decay is illustrated graphically in Fig.3 for varying
362 contributions of Chernobyl fallouts to the total deposit (i.e. ϑ = 0.0, 0.25, 0.5, 1.0). Regardless
363 of ϑ value, results show that the predicted percentage of bioavailable ^{137}Cs in soil at present
364 year (i.e. 2020) is actually very low (D = 0.1 %, 0.17 %, 0.23 %, 0.4 % for ϑ = 0.0, 0.25, 0.5,
365 1.0 respectively). The contribution of Chernobyl to the bioavailable radiocesium present in
366 soil is thus 4 times higher than that of the global fallouts (by excluding the effects of other
367 environmental processes and radioactivity decay). On the other hand, the date of the global
368 fallout deposit appears to have a negligible impact on the predicted value. Results further
369 show that the predicted D's attributed to the global fallout (i.e. ϑ = 0.0) is almost the same
370 whether deposit occurs in 1960 or 1965 (0.10 % versus 0.13 % respectively). This finding
371 suggests, thus, setting the deposition of ^{137}Cs from global fallout to a punctual deposit in the
372 modeling studies of long term ^{137}Cs fate.

373

374

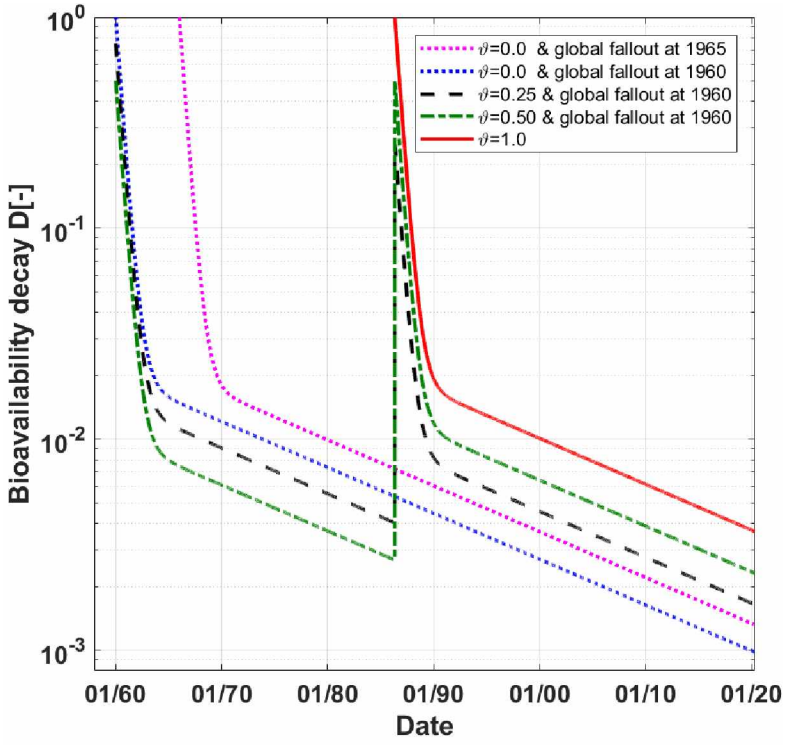

Fig 3: Illustration of changes in radiocesium bioavailable fraction (*D*) in a pasture soil for different levels of contribution of Chernobyl fallouts to the total deposit (i.e. ϑ = 0.0, 0.25, 0.5, 1.0). Except the magenta pointed line, the simulations were performed by assuming a punctual contamination by global fallout occurring at the early 1960. The magenta pointed line illustrates the case of a complete punctual contamination by global fallout (i.e. ϑ =0) occurring in 1965. Constant values (P_{fast}, k_{fast}, k_{slow}) are those obtained by approach 2 (Table 2).

3.2. Exploratory analysis of *TFs* data

To determine whether *TFs* significantly vary among the different areas we performed ANOVA, Turkey's multiple comparison analysis of the log transformed data (Fig S1). The statistical test showed no significant difference between Jura and NPP (*p*-value= 0.94 > 0.05). In contrast, a significant difference was found between Puy de Dôme and the other two areas (*p*-value= 0.006 and 0.009 respectively). Such results would be partly explained on the basis of the soil organic matter (OM) content. This latter was significantly higher in Puy de Dôme compared to Jura and NPP (i.e. 63% of samples are with OM content equal or greater than 20% versus only 16% and 4% for Puy de Dôme, Jura and NPP respectively). The mean

391 observed *TFs* have decreased in the same order: Puy de Dôme (*TF*=0.052) > Jura (*TF*=0.036)
392 > NPP (*TF*=0.032). These observations are consistent with previous studies reporting an
393 increase of ^{137}Cs transfer to plant with increasing OM contents (Noordijk et al., 1992; Rosén
394 et al., 1999).

395 As indicated in Table S3, the observed *TFs* -ranged from 0.003 to 0.18 with a mean value of
396 0.035. This range is close to the lower bound of the range reported by IAEA for pasture
397 stems and shoots and the "all soils" group, i.e. *TFs* values within the range 0.01 - 5 and a
398 mean value of 0.25 (IAEA-TECDOC-472, 2010). Such low observed *TFs* might be explained
399 by the reduction of ^{137}Cs bioavailability with increasing elapsed time since the initial
400 deposition. Indeed, while data compiled by IAEA were mostly relied on studies carried a few
401 years after Chernobyl accident, the present data were collected from 20 to 30 years after
402 Chernobyl and more than 50 years after global fallouts. As indicated in Fig. 3, one would note
403 that even for a site exclusively contaminated b by Chernobyl (i.e. ϑ=1), the bioavailability
404 fraction predicted 20 to 30 years after deposition is 0.7 % and 0.4 % respectively which are
405 actually very much lower than 100. Hence the current low *TFs* with respect to the range
406 compiled by IAEA is accounted by the diminishing of the soil bioavailability, more than 30
407 years after the contamination.

408 **3.3. Predicted versus observed *TFs***

409 Scatter diagrams showing modeled against observed *TFs* for models (M3, M6 and M9 are
410 shown in Fig 4. Results for the remaining models are presented in Fig S2 in SI. Table 3
411 summarizes the averages and the confidence intervals of *CF* and *Kd* estimates for the various
412 models (see section 2.3.2). Since *D* estimates do not differ between models, they are not
413 presented here. Among the 101 observations, its value ranged from 0.001 to 0.005, with a
414 median at 0.004.

415

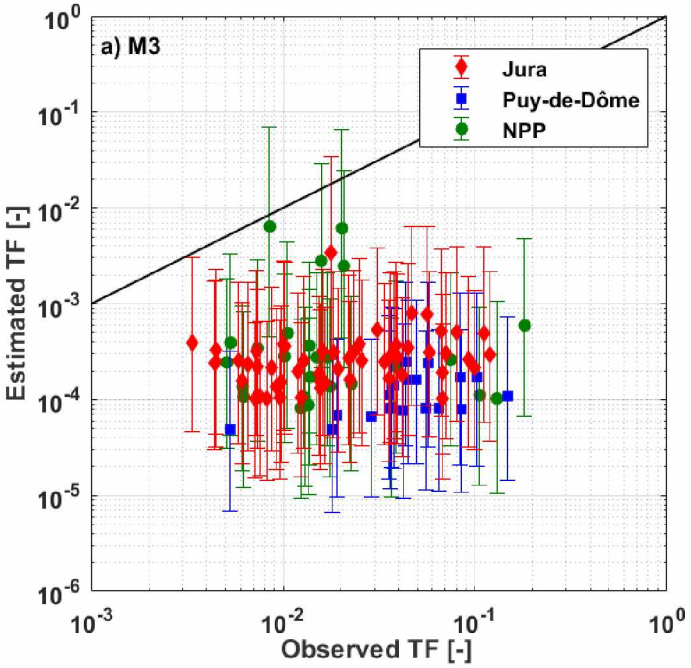
a) M3
Jura
Puy-de-Dôme
NPP
Estimated TF [-]
Observed TF [-]
10^{0}
10^{-1}
10^{-2}
10^{-3}
10^{-4}
10^{-5}
10^{-6}

416

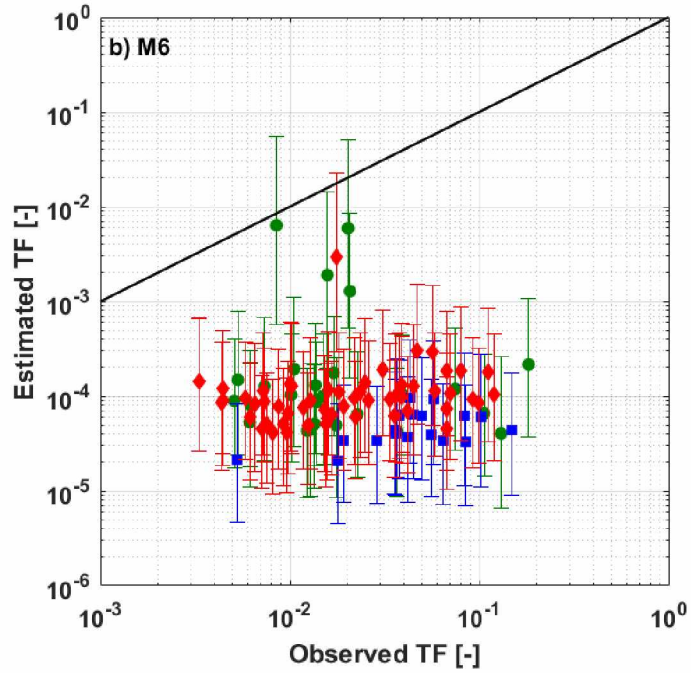
b) M6
Estimated TF [-]
Observed TF [-]
10^{0}
10^{-1}
10^{-2}
10^{-3}
10^{-4}
10^{-5}
10^{-6}

417

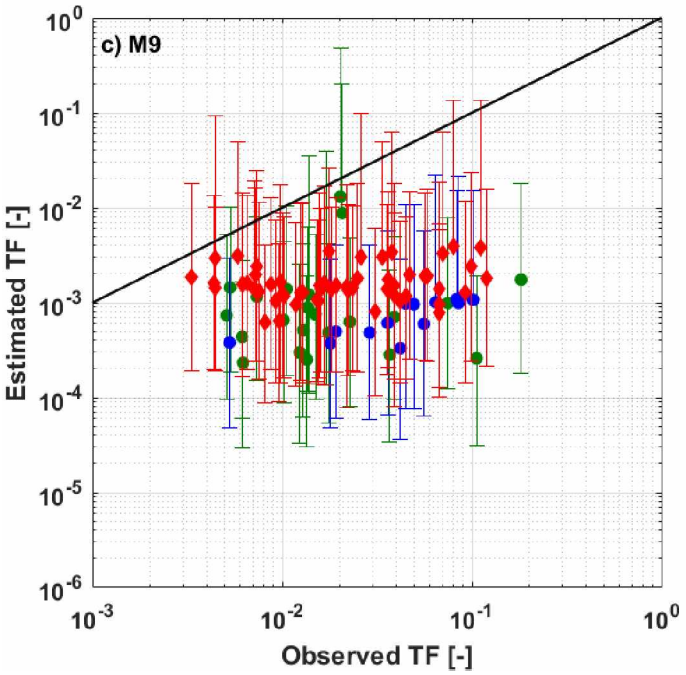

418

419 **Fig 4**: Predicted (95 CI.) versus observed value of the soil-to-grass transfer factor *TF* for the 101
420 samples using: a) model 3, b) model 6, c) model 9. Solid line represents the 1:1 relationship.

421 Thereafter we use the results of the nine models to evaluate their performances by
422 differentiating three families of models: the "original" ones (Absalom et al. (1999), Absalom
423 et al. (2001) and Tarsitano et al. (2011)), the ones based on a *CF* estimated by Smolders et al.,
424 (1997) and the last 3 ones based on RIP^{soil} estimated by Uematsu et al. (2015).

425 *Original models M1, M2 and M3*

426 Table 4 summarizes the statistics of the performances of the tested models. In general terms,
427 results show that the 3 models are as bad as each other in replicating the observations. M2
428 shows a slightly better agreement with observations as confirmed with *Contained* index of
429 56%. Nevertheless, a very poor agreement between observed and predicted *TFs* could still be
430 appeared. Fig 4a clearly illustrates that the *TFs* estimates by M3 are almost 2 orders of
431 magnitude lower than the observed ones. Additionally, no improvement could be found in
432 terms of model ability to describe the variability among sampling soils.

433 *Models based on CF from Smolders et al. (1997): M4, M5 and M6*

434 Results show that application of this parameterization of *CF* leads to a poorer clustering
435 around the 1:1 line than the previous models because the estimated *CFs* were generally lower
436 than those estimated by the original models by a factor of 2 in average (Fig 4b and Table 3).
437 The variability between the sites is also not better explained with these alternative models as
438 confirmed with the poor correlation coefficients (Table 4).

439 *Models based on a RIPsoil from Uematsu et al. (2015): M7, M8 and M9*

440 Results show that using the radiocesium interception potential (RIP^{soil}) for *Kd* calculation has
441 significantly improved the model fits when compared to the previous ones. This improvement
442 is ascribed to the large reduction in *Kd* values of about ~ 5-7 times compared to the original
443 formulations. The relatively high value of 95 % for *Contained* index obtained by M8 is
444 attributable to the high uncertainty in model outputs due to the high uncertainty associated
445 with the input parameters of the corresponding models. Among all the models, the best
446 clustering around the 1:1 line was found in M9 with a $\overline{sim}$/obs ratio of 0.06. However, the
447 matching remains very poor and unconvincing. The relatively high correlation (r=0.76)
448 observed for Puy de Dôme sites is likely due to the number of observations which was smaller
449 than in other cases (N=13 compared to N=19). Indeed, application of Uematsu's
450 parameterization to these sites produced some negative values for 3 and 7 samples from NPP
451 and Puy de Dôme respectively, suggesting that this equation which was calibrated for
452 Japanese soils might not be suitable for European soils.

453 To summarize, we would say that, while the observed *TF* display a wide range of variability
454 (by a factor of 30, typically), the predicted *TF* do not vary significantly among sites, and
455 remain relatively constant for a given region (Jura, Puy de Dôme, NPP). This demonstrates
456 that the variability was poorly explained by any of these 9 models, although slightly better in

457 Puy de Dôme region. The second important result is that predicted *TFs* are systematically
458 biased, and remain far below the observed ones, by one to two orders of magnitude, typically.
459 These results argue therefore against the usefulness of the semi-mechanistic models to
460 accurately predict the long-term soil-to-grass transfer of ^{137}Cs in the French pastures under
461 investigation.

462 **Table 3**: Summary of *CF* and *Kd* values calculated with the various models

Model	Description	*CF* (L/kg$_{dm}$)	*Kd* (L/kg$_{dm}$)
M1[a,b]	*CF* (Absalom et al., 1999) *Kd* (Absalom et al., 1999)	$\overline{[2.7x\ 10^1 - 3.0x\ 10^4]}$ $\overline{5.5\ x\ 10^2}$	$\overline{[6.1x\ 10^2 - 3.5\ x\ 10^5]}$ $\overline{4.8\ x\ 10^4}$
M2[a,b]	*CF* (Absalom et al., 2001) *Kd* (Absalom et al., 2001)	$\overline{[1.9x\ 10^1 - 1.2x\ 10^4]}$ $\overline{2.6\ x\ 10^2}$	$\overline{[8.6x\ 10^2 - 2.3\ x\ 10^4]}$ $\overline{1.0\ x\ 10^4}$
M3[a,b]	*CF* (Tarsitano et al., 2011) *Kd* (Tarsitano et al., 2011)	$\overline{[7.0\ x10^1 - 4.8\ x\ 10^4]}$ $\overline{7.4\ x\ 10^2}$	$\overline{[9.3\ \text{x}\ 10^2 - 4.8\ x10^4]}$ $\overline{1.5\ x\ 10^4}$
M4[a,b]	*CF* (Smolders et al., 1997) *Kd* (Absalom et al., 1999)	$\overline{[6.3\ x10^1 - 5.9x10^3]}$ $\overline{3.0\ x\ 10^2}$	$\overline{[6.1\ x10^2 - 3.5\ x10^5]}$ $\overline{4.8\ x\ 10^4}$
M5[a,b]	*CF* (Smolders et al., 1997) *Kd* (Absalom et al., 2001)	$\overline{[\ 3.8\ x10^1 - 4.0\ x10^4]}$ $\overline{2.6\ x\ 10^2}$	$\overline{[\ 8.6\ x10^2 - 2.3\ x\ 10^4]}$ $\overline{1.0\ x\ 10^4}$
M6[a,b]	*CF* (Smolders et al., 1997) *Kd* (Tarsitano et al., 2011)	$\overline{[\ 4.9\ x10^1 - 4.6\ x10^4]}$ $\overline{2.7x\ 10^2}$	$\overline{[9.3\ x10^2 - 4.8\ x10^4]}$ $\overline{1.5\ x\ 10^4}$
M7[a,c]	*CF* (Absalom et al., 1999) RIP_{soil} (Uematsu et al., 2015) *Kd*= RIP_{soil} /mk	$\overline{[\ 2.7\ x10^1 - 3.0\ x\ 10^4]}$ $\overline{6.4\ x\ 10^2}$	$\overline{[5.2\ x10^2 - 4.4\ x\ 10^4]}$ $\overline{6.5\ x\ 10^3}$
M8[a,c]	*CF* (Absalom et al., 2001) RIP_{soil}(Uematsu et al., 2015) *Kd*= RIP_{soil} /mk	$\overline{[\ 1.9\ x10^1 - 9.6\ x\ 10^3]}$ $\overline{2.3\ x\ 10^2}$	$\overline{[2.2\ x10^2 - 3.5\ x\ 10^4]}$ $\overline{2.1\ x\ 10^3}$
M9[a,c]	*CF* (Tarsitano et al., 2011) RIP_{soil} (Uematsu et al., 2015) *Kd*= RIP_{soil} /mk	$\overline{[7.0\ x10^1 - 4.5x\ 10^4]}$ $\overline{9.3\ x\ 10^2}$	$\overline{[\ 1.8\ x10^2 - 5.3\ x\ 10^4]}$ $\overline{2.8\ x\ 10^3}$

463 [a] Median values are overlined while 95CI values are given in brackets
464 [b] Number of observations n=101
465 [c] Number of observations n=92

Table 4: Model performance indexes for predicted *TF*

Statistic	Site	Models								
		M1[a]	M2[a]	M3[a]	M4[a]	M5[a]	M6[a]	M7[b]	M8[b]	M9[b]
r	NPP	-0.13	-0.01	-0.1	-0.04	-0.03	-0.09	-0.06	0.16	0.07
	Puy de Dôme	0.52	0.53	0.54	0.34	0.52	0.50	0.67	0.70	0.76
	Jura	0.29	0.29	0.24	0.31	0.27	0.21	0.15	0.10	0.15
	All	-0.07	0.05	-0.04	-0.02	0.02	-0.05	-0.05	0.08	0.06
Contained (%)	NPP	0.0	61.5	15.8	0.0	11.5	7.7	8.7	91.3	34.8
	Puy de Dôme	0.0	10.5	0.0	0.0	0.0	0.0	0.0	84.6	0.0
	Jura	0.0	69.6	1.8	0.0	0.0	1.8	0.0	100	37.5
	All	0.0	56.4	5.0	0.0	3.0	3.0	2.2	95.7	31.5
ratio $\overline{sim}$/obs (-)	NPP	0.007	0.0064	0.0168	0.0039	0.0075	0.0077	0.0124	0.0161	0.05
	Puy de Dôme	0.0004	0.0010	0.0027	0.0004	0.0012	0.0012	0.0029	0.0064	0.02
	Jura	0.0023	0.0047	0.0124	0.0012	0.0050	0.0047	0.0230	0.0237	0.08
	All	0.002	0.0037	0.0093	0.0011	0.0041	0.0038	0.0175	0.0193	0.06

[a] Number of observations n=101

[b] Number of observations n=92

3.4. Why models did not fit well the observed data?

Assuming that the bioavailability decay (*D*) has been accurately estimated thanks to the calibration procedure, the low performances of the models could be attributed to the inaccurate estimations of the *CF/Kd* ratio as part of equation (2). Several factors may have deteriorated the estimates. At first, being semi-empirical models, the use of these models is usually restricted to the specified (grass and/or soil) data to which they were calibrated. An extrapolation to other data/sites may result in wrong estimates. An adjustment of their default parameters might, thus, be required each time we change sites or of data. Additionally, these models have been mostly calibrated by laboratory data of specific plant species especially ryegrass and wheat which it is not the case here where a large variety of herbage species was observed from a sampling plot to another (i.e. such as *poaceae, fabaceae, ranunculaceae and asteraceae*) (Besson, 2009). This variability is mostly due to the variability of soil characteristics and climatic conditions. Several studies have highlighted significant differences in plant uptake of radiocesium among the plant species (Broadley and Willey, 1997; Ciuffo et al., 2003; Lasat et al., 1997). It is possible, therefore, that a significant part of the observed variability originates in *CF* due to the variety of grass species encountered at the monitoring sites. Another weakness of the models, is that the process of adherence of contaminated soil particles to the aerial part of the vegetation, which has been reported to increase significantly the radiocesium content in grass (Beresford and Howard, 1991), is neglected in the models under consideration.

Another important reason explaining the discrepancy between observed and predicted *TF* is the extremely high estimated *Kd* values, the median values of which range from 2100 to 48000 L/kg_{dm} (Table 3). Indeed, the predicted *Kd* values are calculated using semi-empirical equations based on linear correlations which were derived from non-labile *Kd* measurements. These measurements are based on the hypothesis that radiocesium in solution is in

494 instantaneous equilibrium with the solid phase of soil and that the exchanges between these
495 phases is reversible. However, a fraction of radiocesium may become fixed to the solid phase
496 due to ageing effects. This may lead to non-labile *Kd* values higher by orders of magnitude
497 than the labile ones. This was shown in Fig 3 where the labile fraction rapidly decreased after
498 initial deposition due to the rapid decrease of bioavailability in the first few weeks to months
499 after initial contamination. Results showed that a decrease by more than 98% of the initial
500 labile fraction would occur after only 44 months following Chernobyl accident, even in the
501 case of unique source of contamination by Chernobyl.
502 To test this assumption, we carried out additional simulations adopting a constant labile *Kd*
503 value of 165 L/kg_{dm} as recommended by Roussel-Debet and Colle (2005). The test was
504 applied on the first six models (i.e. M1, M2, M3, M4, M5, M6). The models M7, M8, and M9
505 were not included here as they were essentially based on the estimation of *Kd* using RIP^{soil}
506 equation. Results obtained with models M3 are displayed in Fig. 4, while the remaining ones
507 are displayed in Fig S3 in S.I. Table 5 shows that the best clustering around the 1:1 line was
508 found with M3 with a ratio $\overline{sim}/obs$ value of 0.97. Compared to the former models, results
509 show that the modification of labile *Kd* has significantly improved the model performances.
510 However, no improvement could be found regarding the variability. This is not surprising
511 since a single value of labile *Kd* was imposed for all the sampled soils.
512
513

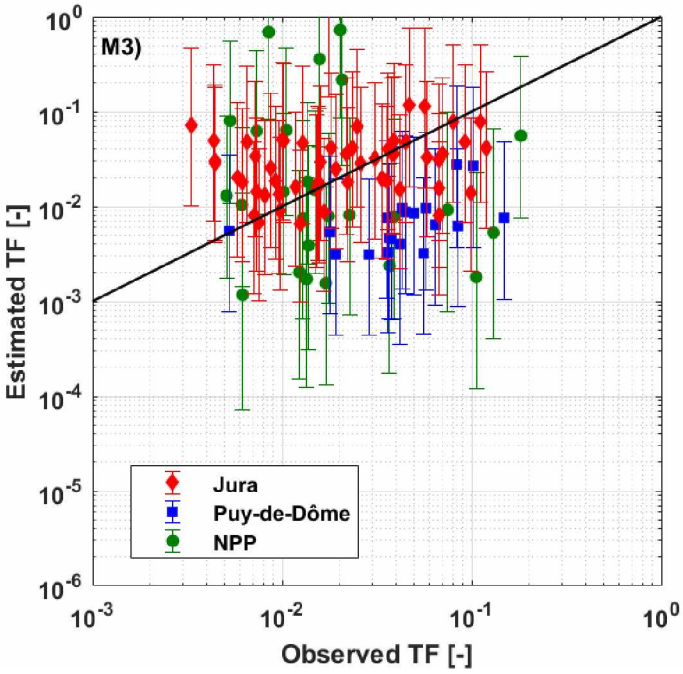

514

515 **Fig 5**: Predicted (95 CI) versus observed value of the soil-to-plant transfer factor *TF* for the 101

516 samples, using model M3 with an imposed labile *Kd* value of 165 L/kg$_{dm}$. Solid line represents the

517 1:1 relationship.

518 **Table 5**: Model performance indexes for predicted *TF* with an imposed labile *Kd* value of 165

519 L/kg$_{dm}$

Statistic	site	Models					
		M1	**M2**	**M3**	**M4**	**M5**	**M6**
r	**NPP**	-0.19	-0.05	-0.14	-0.18	-0.06	-0.15
	Puy de Dôme	0.35	0.53	0.47	0.34	0.54	0.47
	Jura	0.14	0.21	0.16	0.12	0.20	0.14
	All	-0.13	0.01	-0.08	-0.14	-0.01	-0.09
Contained (%)	**NPP**	42.3	100	61.5	42.3	38.6	30.8
	Puy de Dôme	5.3	100	57.9	5.3	5.3	5.3
	Jura	71.4	100	87.5	64.3	62.5	69.6
	All	51.5	100	75.3	47.5	45.5	47.5
ratio $\overline{sim}$/obs (-)	**NPP**	0.38	0.14	0.52	0.42	0.17	0.20
	Puy de Dôme	0.06	0.07	0.16	0.06	0.08	0.06
	Jura	1.04	0.34	1.23	0.52	0.37	0.47
	All	0.66	0.24	0.97	0.36	0.28	0.37

520

521

522 # 4. Conclusion

523 With the aim in mind of improving our understanding of the long-term behavior of ^{137}Cs in
524 terrestrial environments, the present paper evaluates existing assessment models against long-
525 term monitoring data of activity levels observed -between 2004 and 2017- in different French
526 grazing areas contaminated by global fallouts and Chernobyl accident. The observed soil to
527 grass transfer factor values (*TFs*) were found to be close to the lower bound of those
528 synthesized by IAEA and this was explained by the extreme reduction of ^{137}Cs bioavailability
529 due to the old contamination of monitoring sites. For this reason, an effort has been carried
530 out to better quantify the decay of bioavailable radiocesium in soil, using mid-term (10 years
531 about) and long term (more than 20 years) series of ^{137}Cs activities in milk observed in 4
532 European countries after Chernobyl. These enable us to identify a double kinetics of
533 bioavailability decay with two effective half-lives for the fast and slow declining fractions
534 which were found to be equal to 0.46±0.11 yr and 9.57±1.12 yr respectively. Additionally, a
535 very high value around 0.97 was identified for the fast-declining fraction (P_{fast}). A special
536 attention should have been be paid to bioavailability decay (D) not only because inaccurate
537 estimate of this parameter might lead to significant overestimate of ^{137}Cs transfer from soil to
538 grass and thereby in the food chain but also because D would explain a large part of the
539 variability observed on *TFs* in literature. However, In spite of this effort, predicted *TFs*
540 remain by far lower than the observed ones by one to two orders of magnitude typically,
541 suggesting that *Kd* is overestimated by models. Thus, calculation of *Kd* should involve easily
542 exchangeable ^{137}Cs rather than total soil ^{137}Cs. This is all the more justified that the non-
543 exchangeable fraction (i.e. non-labile and non-bioavailable) was already taken into account
544 through *D (Fig 3)*, and therefore *Kd* has only to concern the easily exchangeable part (labile
545 and bioavailable). Furthermore, the variability between sites was poorly explained by semi-
546 mechanical models mostly because, being semi- empirical models, they require a recalibration
547 of the parameters and coefficients involved in the model each time we change sites or of data.

5. Acknowledgements

This work was funded by Institut de Radioprotection et de Sûreté Nucléaire (IRSN) in France, MEMOREX project. The field work on radiocesium monitoring at some French pasture sites was undertaken during the PhD program of Benoit Besson. The authors are grateful to Gilles Salaün for help in data collection. The first author thanks Dr. Marie Simon-Cornu (IRSN) for reviewing the manuscript prior to submission.

6. References

Absalom, J.P., Young, S.D., Crout, N.M.J., 1995. Radio- caesium fixation dynamics: measurement in six Cumbrian soils. Eur. J. Soil Sci. 46, 461–469. https://doi.org/10.1111/j.1365-2389.1995.tb01342.x

Absalom, J.P., Young, S.D., Crout, N.M.J., Nisbet, A.F., Woodman, R.F.M., Smolders, E., Gillett, A.G., 1999. Predicting soil to plant transfer of radiocesium using soil characteristics. Environ. Sci. Technol. 33, 1218–1223.

Absalom, J.P., Young, S.D., Crout, N.M.J., Sanchez, A., Wright, S.M., Smolders, E., Nisbet, A.F., Gillett, A.G., 2001. Predicting the transfer of radiocaesium from organic soils to plants using soil characteristics. J. Environ. Radioact. 52, 31–43.

Albers, B.P., Steindl., H., Schimmack., W., Bunzl., K., 2000. Soil-to-plant and plant-to-cow' s milk transfer of radiocaesium in alpine pastures : significance of seasonal variability. Chemosphere 41, 717–723.

Almahayni, T., Beresford, N.A., Crout, N.M.J., Sweeck, L., 2019. Fit-for-purpose modelling of radiocaesium soil-to-plant transfer for nuclear emergencies: a review. J. Environ. Radioact. 201, 58–66. https://doi.org/10.1016/j.jenvrad.2019.01.006

571 Beresford., N.A., Howard., B.J., 1991. The importance of soil adhered to vegetation as a
572 source of radionuclides ingested by grazing animals. Sci. Total Environ. 107, 237–254.
573 https://doi.org/10.1016/0048-9697(91)90261-C

574 Besson, B., 2009. Sensibilité radioécologiques des zones de prairie permanentes. PhD thesis.
575 Université de Franche-Comté Besançon, France.

576 Brimo, K., Gonze, M.A., Pourcelot, L., 2019. Long term decrease of 137Cs bioavailability in
577 French pastures : Results from 25 years of monitoring Long term decrease of 137 Cs
578 bioavailability in French pastures : Results from 25 years of monitoring. J. Environ.
579 Radioact. 208–209. https://doi.org/10.1016/j.jenvrad.2019.106029

580 Broadley, M.R., Willey, N.J., 1997. Differences in root uptake of radiocaesium by 30 plant
581 taxa. Environ. Pollut. 97, 11–15.

582 Brown, J., Dvarzhak, A., 2019. EJP-CONCERT: D9.61- Guidance to select level of
583 complexity.

584 Ciuffo, L., Velasco, H., Belli, M., Sansone, U., Transfer, S., 2003. Cs soil-to-plant transfer for
585 individual species in a semi-natural grassland . Influence of potassium soil content. J.
586 Radiat. Res. 283, 277–283.

587 Duffa, C., Masson, M., Gontier, G., Claval, D., Renaud, P., 2004. Synthèse des études
588 radioécologiques annuelles menées dans l environement des centrales électronucléaires
589 francaises deupuis 1991. Radioprotection 39, 233–254.

590 Frissel, M., Deb, D., Fathony, M., Lin, Y., Mollah, A., Ngo, N., Othman, I., Robison, W.,
591 Skarlou-Alexiou, V., Topcuoğlu, S., Twining, J., Uchida, S., Wasserman, M., 2002.
592 Generic values for soil-to-plant transfer factors of radiocesium. J. Environ. Radioact. 58,
593 113–128.

IAEA-TECDOC-472, 2010. Handbook of parameter values for the prediction of radionuclide transfer in terrestrial and freshwater. Vienna.

Lasat, M.M., Norvell, W.A., Kochian, L. V, 1997. Potential for phytoextraction of137 Cs from a contaminated soil. Plant Soil 195, 1997.

Mück, K., 2003. Sustainability of radiologically contaminated territories. J. Environ. Radioact. 65, 109–130. https://doi.org/10.1016/S0265-931X(02)00091-7

Noordijk, H., Van Bergeijk, K.E., Lembrechts, J., Frissel, M.J., 1992. Impact of ageing and weather conditions on soil-to-plant transfer of radiocesium and radiostrontium. J. Environ. Radioact. 15, 277–286.

Renaud, R., Louvat, D., 2004. Magnitude of fission product depositions from atmospheric nuclear weapon test fallout in France. Health Phys. 86, 353–8. https://doi.org/10.1097/00004032-200404000-00003

Rosén, K., Öborn, I., Lönsjö, H., 1999. Migration of radiocaesium in Swedish soil profiles after the Chernobyl accident, 1987–1995. J. Environ. Radioact. 46, 45–66.

Roussel-Debet, S., Colle, C., 2005. Comartement de radionucléides (Cs, I, Sr, Se, Tc) dans le sol: proposition de valeurs de Kd par défaut. Radioprotection 40, 203–229.

Roussel-Debet, S., Renaud, P., Métivier, J., 2007. 137Cs in French soils : Deposition patterns and 15-year evolution. Sci. Total Environ. 374, 388–398. https://doi.org/10.1016/j.scitotenv.2006.12.037

Smith, J.T., Fesenko, S. V., Howard, B.J., Horrill, A.D., Sanzharova, N.I., Alexakhin, R.M., Elder, D.G., Naylor, C., 1999. Temporal change in fallout 137Cs in terrestrial and aquatic systems : A whole ecosystem approach. Environ. Sci. Technol. 33, 49–54.

https://doi.org/10.1021/es980670t

Smolders, E., Van Den Brande, K., Merckx, R., 1997. Concentrations of 137Cs and K in soil solution plant availability of 137Cs in soils. Environ. Sci. Technol. 31, 3432–3438. https://doi.org/10.1021/es970113r

Tarsitano, D., Young, S.D., Crout, N.M.J., 2011. Evaluating and reducing a model of radiocaesium soil-plant uptake. J. Environ. Radioact. 102, 262–269. https://doi.org/10.1016/j.jenvrad.2010.11.017

Uematsu, S., Smolders, E., Sweeck, L., Wannijn, J., Hees, M. Van, Vandenhove, H., 2015. Predicting radiocaesium sorption characteristics with soil chemical properties for Japanese soils. Sci. Total Environ. 524–525, 148–156. https://doi.org/10.1016/j.scitotenv.2015.04.028

Vrugt, J.A., 2016. Markov chain Monte Carlo simulation using the DREAM software package: Theory, concepts, and MATLAB implementation. Environ. Model. Softw. 75, 273–316. https://doi.org/10.1016/j.envsoft.2015.08.013

Wright, S.M., Smith, J.T., Beresford, N.A., Scott, W.A., 2003. Monte-Carlo prediction of changes in areas of west Cumbria requiring restrictions on sheep following the Chernobyl accident. Radiat. Environ. Biophys. 42, 41–47.

Yamamura, K., Fujimura, S., Ota, T., Ishikawa, T., Saito, T., Arai, Y., Shinano, T., 2018. A statistical model for estimating the radiocesium transfer factor from soil to brown rice using the soil exchangeable potassium content. J. Environ. Radioact. 195, 114–125.